

# Design and performance evaluation of the six-row side deep fertilizer applicator for paddy fields

Kemoh Bangura<sup>1,2,3</sup>, Shuanglong Wu<sup>1</sup>, Zhenyu Tang<sup>1</sup>, Xiao Feng<sup>1</sup>, Renjun Hu<sup>1</sup>, Yinghu Cai<sup>1</sup>, Yuhao Zhou<sup>1</sup>, Zhanpeng Liang<sup>1</sup>, Zhiwei Zeng<sup>4</sup>, Abdulai Bangura<sup>1,2</sup>, Ernest Owusu-Sekyere<sup>5</sup>, Long Qi<sup>1,5,6</sup>, Hao Gong<sup>1\*</sup>

(1. College of Engineering, South China Agricultural University, Guangzhou 510642, China;

2. Sierra Leone Agricultural Research Institute (SLARI)/Rokupr Agricultural Research Center (RARC), Freetown, Sierra Leone;

3. Department of Agricultural Engineering, School of Technology, Njala University, Sierra Leone;

4. Department of Agricultural Engineering Technology, University of Wisconsin-River Falls, WI 54022, USA;

5. Department of Biosystems Engineering, University of Manitoba, Winnipeg, Manitoba, Canada;

6. State Key Laboratory of Agricultural Equipment Technology, Guangzhou 510642, China)

**Abstract:** Deep application of chemical fertilizer is an alternative method to improve the fertilizer utilization efficiency of directly seeded and transplanted rice and minimize the adverse effects of fertilizer on the environment. Different fertilization machines have been introduced for fertilizer deep placement. However, machines for this purpose have not been widely accepted due to the problem of inconsistent performance in applications. In response to this problem, this study developed a six-row deep fertilizer applicator with an improved discharge device. The structural design of the discharge device was optimized, and field performance experiments were conducted on the entire machine. First, a single row operation model of the fertilizer applicator was established based on the Discrete Element Method (DEM). Three spiral grooved wheel speeds were used to test the uniformity and accuracy of fertilization. The optimization test results showed that the spiral grooved wheel has good fertilizer discharge effect at a speed of 40 r/min, a groove radius of 6 mm, a grooved wheel working length of 50 mm, and a grooved wheel spiral angle of 45°. The coefficient of variation of fertilizer application uniformity under these parameter settings was 6.30%. Field experiments were conducted to test the machine's performance under static and dynamic conditions. The static test results showed that the consistency and stability variations of fertilization in each row were less than 5%. When the expected fertilization rates were 150, 225, 300, and 375 kg/hm<sup>2</sup>, the fertilization accuracy of the six-row fertilization machine was 95.5%, and the overall deviation from the actual fertilization rates was less than 5%. The study provides a new tool for the advancement of rice fertilization technology and lays a research foundation for the development of efficient and precise rice fertilization machinery.

**Keywords:** deep fertilization device, structural design, DEM simulation, field experiment

**DOI:** [10.25165/ijabe.20241706.8598](https://doi.org/10.25165/ijabe.20241706.8598)

**Citation:** Bangura K, Wu S L, Tang Z Y, Feng X, Hu R J, Cai Y H, et al. Design and performance evaluation of the six-row side deep fertilizer applicator for paddy fields. *Int J Agric & Biol Eng*, 2024; 17(6): 156–165.

## 1 Introduction

At present, China's population is growing, the problem of food security is becoming increasingly serious, and increasing food production has become a national priority. The application of chemical fertilizer is one of the main ways to increase food production. In the rice planting process, for example, the right amount of fertilizer application can effectively increase rice yield<sup>[1-3]</sup>. But throughout the farming process, our farmers use far more fertilizer than necessary. Currently, China has one of the highest rates of chemical fertilizer use, with fertilizer being applied to 67%

of grain crops<sup>[4,5]</sup>.

The most common traditional practice of applying fertilizer to rice fields in China is surface broadcasting. There are several disadvantages to broadcasting. First, when fertilizer is broadcast in rice fields, about 30%-35% of the fertilizer is lost through surface runoff, evaporation, and being washed down into the soil; this leads to wastage of fertilizer<sup>[6-8]</sup>. On the other hand, broadcasting fertilizer is more expensive than deep placement, and it is commonly done 2-3 times per season<sup>[5]</sup>. Also, under fertilizer broadcasting conditions, the uniformity of fertilizer distribution in the field is very poor, so that the absorption and utilization rate of rice seedlings differ

**Received date:** 2023-10-17 **Accepted date:** 2024-10-24

**Biographies:** **Kemoh Bangura**, PhD, research interest: agricultural machinery and implement, Email: [bangura.kemoh@gmail.com](mailto:bangura.kemoh@gmail.com); **Shuanglong Wu**, Associate Professor, research interest: intelligent agricultural machinery equipment, Email: [wushuanglong@scau.edu.cn](mailto:wushuanglong@scau.edu.cn); **Zhenyu Tang**, PhD candidate, research interest: machine-soil-crop system simulation, Email: [tangzhenyu2019@163.com](mailto:tangzhenyu2019@163.com); **Xiao Feng**, Associate Professor, research interest: intelligent agricultural machinery, Email: [fengxiao@scau.edu.cn](mailto:fengxiao@scau.edu.cn); **Renjun Hu**, Associate Professor, research interest: electrification and intellectualization of agriculture, Email: [rjhu@scau.edu.cn](mailto:rjhu@scau.edu.cn); **Yinghu Cai**, M.Eng, research interest: tea intelligent picking, Email: [yinghucai@163.com](mailto:yinghucai@163.com); **Yuhao Zhou**, PhD candidate, research interest: rice phenotype, Email: [zyh31st@163.com](mailto:zyh31st@163.com); **Zhanpeng Liang**, M.Eng, research

interest: robot, Email: [957894146@qq.com](mailto:957894146@qq.com); **Zhiwei Zeng**, Associate Professor, research interest: discrete element method and biomaterials, Email: [zhiwei.zeng@uwrf.edu](mailto:zhiwei.zeng@uwrf.edu); **Abdulai Bangura**, MSc, research interest: design and experiment of laser leveler, Email: [abdulaibags@yahoo.com](mailto:abdulaibags@yahoo.com); **Ernest Owusu-Sekyere**, PhD candidate, research interest: machine-soil modeling and simulation, Email: [esekyere82@gmail.com](mailto:esekyere82@gmail.com); **Long Qi**, Professor, research interest: smart agriculture, agricultural robots and machine vision. Email: [qilong@scau.edu.cn](mailto:qilong@scau.edu.cn).

**\*Corresponding author:** **Hao Gong**, Associate Professor, research interest: mechanism of seed soil interaction. College of Engineering, South China Agricultural University, Guangzhou 510642, China. Tel: +86-18774057818, Email: [GongHao@scau.edu.cn](mailto:GongHao@scau.edu.cn).

greatly and ultimately affect rice growth, panicle formation, yield, and quality<sup>[9-11]</sup>. Therefore, how to improve fertilizer use efficiency has become a national concern<sup>[6,12]</sup>. One of the ways to improve the efficiency of using chemical fertilizers is through the development and promotion of improved fertilizer application devices to replace the conventional fertilizer application methods for better uniformity of fertilizer application. Fertilization uniformity refers to the uniform fertilizer distribution during the operation of the fertilizer applicator<sup>[10,13]</sup>. Uniformity can make the fertilizer better distributed in the root zone and improve the utilization efficiency of nutrients.

Research reports have shown that, compared to surface fertilization, the use of improved fertilizer discharge devices for deep application of fertilizers between 4.5-7.0 cm of soil depth can improve grain yield and fertilizer utilization efficiency<sup>[6,14-16]</sup>. Specifically, comparative studies were conducted between deep fertilizer application and surface fertilization methods under the same fertilizer rates<sup>[1,2,9,10,17,18]</sup>. The results of these studies showed that higher rice production output and greater rice production economic benefits were achieved with deep fertilizer application methods. Also, deep placement of fertilizer encourages line transplanting and makes weeding easier.

Theoretical and experimental investigations on fertilizer discharge devices have been conducted in recent years<sup>[19-27]</sup>. The straight grooved wheel is the most extensively utilized among those created in China for fertilizer discharge due to its benefits, including its straightforward structure, ease of manufacture and processing, and good adaptability<sup>[28-30]</sup>. But the straight grooved wheel faces a number of difficult problems, including poor operation stability, a low discharge mass rate, poor uniformity of fertilizer discharge, and frequent clogging of fertilizer delivery pipelines, resulting in low accuracy of field application<sup>[19,31-33]</sup>. To find a solution to these problems, this study proposes a spiral grooved wheel structure to provide stable, consistent, and accurate fertilizer application rates in the field. It has been noted that the spiral grooved wheel provides good results for the uniformity and mass rate of fertilizer discharge<sup>[23,28,34-36]</sup>. The spiral grooved wheel can also handle fertilizer granules of different sizes and shapes<sup>[20,21,36,37]</sup>. In these existing studies, no on-site experimental studies were conducted to verify the performance and accuracy of the spiral grooved wheel fertilization device. The goal of this research was to close this gap.

The complexity of the fertilizer discharge process, which involves particle mobility and interactions with the machine, makes it challenging to understand fertilizer discharge features through experiments<sup>[38,39]</sup>. To comprehend and see the microscopic interaction between particles and the machine, computer simulation utilizing the discrete element method (DEM) would be a viable option. The DEM has been used in numerous agricultural fields and was thought to be an efficient modeling technique for dealing with particle materials<sup>[31,40-42]</sup>. In recent years, granular fertilizers have been simulated using DEM. DEM was utilized by He et al.<sup>[26]</sup> and Przywara et al.<sup>[37]</sup> to model the discharge of outer grooved wheels. The preliminary findings demonstrated the validity and efficacy of the DEM simulation when the simulated results were compared to the test results. Zhang et al.<sup>[21]</sup> studied the effects of different rotation speeds of an outer groove on a fertilizer discharge device's application uniformity. The results of the bench and field tests aligned with the simulation test. These findings support the effectiveness of DEM and provide a reference and theoretical basis for the design of efficient fertilizer machines. Adilet et al.<sup>[31]</sup> (2023) created a pin-roller fertilizer metering device with spiral grooved wheel to apply fertilizers to the soil. The performance of the devices

was modeled using the DEM. The results showed that the DEM model was able to simulate the spiral grooved wheel fertilizer devices with reasonably good accuracy. Bu et al.<sup>[20]</sup> studied the spreading performance of a centrifugal variable-rate fertilizer applicator by conducting DEM simulation tests. The findings demonstrated that the designed variable-rate spreader had a lower coefficient of variation. Zeng et al.<sup>[39]</sup> developed a fluted-roller fertilizer applicator. The performance of the machine was tested using DEM and experiment. It was deduced from the results that the precision and accuracy of the amount of fertilizer application were improved. These researchers' findings proved that DEM is a useful technique for simulating granular materials. To simulate the fertilizer discharge performance of the spiral grooved wheel designed in this paper, the DEM was employed. At the same forward speed, three spiral grooved wheel speeds were used to test the uniformity and consistency of fertilization. A six-row fertilizer applicator (6RFA) was developed, adopting the spiral grooved wheel structure. Field experiments were conducted to test the whole machine's performance under static and dynamic conditions. The test results showed that the uniformity and accuracy of the developed fertilization machine prototype meet agricultural fertilization standards. This is important, as further research on deep fertilization machines and tools is needed, and this will contribute to the popularization of deep fertilization technology and tools in paddy fields in China.

## 2 Materials and methods

### 2.1 Design of the 6RFA machine

The 6RFA machine consists of the following major parts: fertilizer box, frame, speed control system, DC motor, fertilizer distribution apparatus, discharge shaft, soil opener, and soil leveler. The machine is connected to the tractor body through the suspension frame. The prototype and overall structure of the 6RFA machine are shown in Figures 1 and 2, respectively.



Figure 1 Six-row granular fertilizer applicator prototype

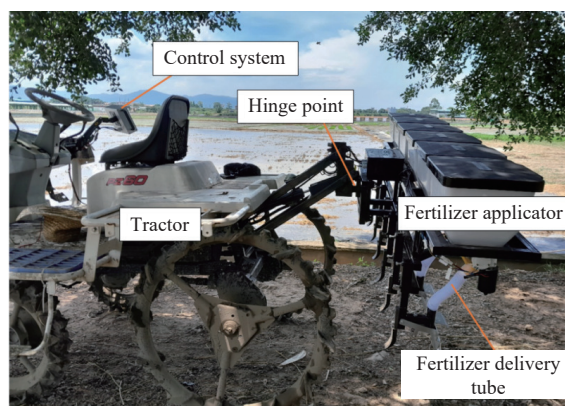


Figure 2 Overall structure of the six-row fertilizer machine

The 6RFA machine was developed based on the spiral grooved wheel structure with a variable rate control system. The technical details of the 6RFA are listed in Table 1.

**Table 1 Technical specification of 6RFA machine**

Project	Parameter
Working width	2.5 m
Number of operating rows	6
Working speed	Varied
Fertilizer application mode	Variable rate
Type of fertilizer apparatus	Spiral grooved wheel fertilizer apparatus

**2.2 Structure and parameter design of the fertilizer discharge model**

The fertilizer discharge model designed consisted of a fertilizer box, a spiral grooved wheel, a discharge box, a discharge shaft, and a fertilizer discharge spout (Figure 3). The working diameter of existing grooved wheels is in the range of 50-65 mm, and the grooved wheel length generally varies from 25 to 50 mm<sup>[28,34,36]</sup>. Based on this, the working diameter and length of the spiral grooved wheel designed in this study were 50 and 48 mm, respectively. In the literature, the groove radius ranges from 2-9 mm, and the number of grooves ranges from 6-10<sup>[21,43]</sup>. Within these ranges, a groove radius (*r*) of 6 mm and a number of grooves (*z*) of 8 were selected. The structure of the improved spiral grooved wheel is shown in Figure 4.

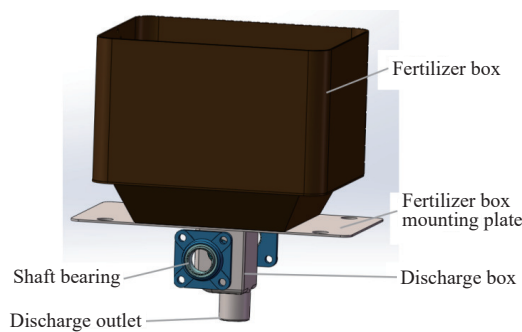


Figure 3 Screenshot of fertilizer discharging device with spiral grooved wheel

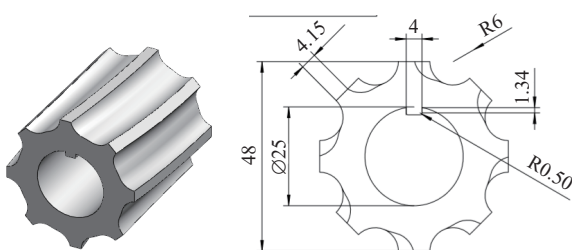


Figure 4 Structure of the spiral grooved wheel

When the fertilizer applicator is in operation, the fertilizer is first filled into the groove of the grooved wheel by gravity<sup>[43]</sup>. Then it is discharged through the rotation of the groove. The spiral grooved wheel is driven by the fertilizer discharge shaft and continuously rotates under the action of various forces. The mass of fertilizer discharge when the grooved wheel rotates one revolution can be calculated by the following equation:

$$q = \frac{SLZ\gamma\rho}{1000} \tag{1}$$

where, *q* is the mass of fertilizer, g/r; *S* is cross-sectional area of a single groove, mm<sup>2</sup>; *L* is the effective working length of the grooved wheel, mm; *Z* is the number of grooves;  $\gamma$  is the filling coefficient of the fertilizer in the groove;  $\rho$  is the fertilizer density, g/cm<sup>3</sup>.

It is evident from Equation (1) that for a particular fertilizer applicator and discharge object, the mass of fertilizer applied per rotation of the grooved wheel is only related to the sectional area *S*, and that the sectional structural parameters and the fertilizer flow and application performance during the fertilizer transport process, from filling to discharge, are inevitably linked<sup>[34,43]</sup>. Figure 5 shows the groove sectional shape<sup>[34]</sup>.

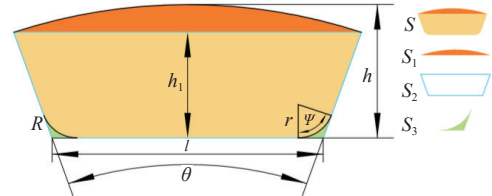


Figure 5 Sectional shape of single groove

The cross-sectional area *S* of a single groove obtained from Figure 5 is:

$$S = S_1 + S_2 - 2S_3 \tag{2}$$

where, *S*<sub>1</sub> is the spherical area; *S*<sub>2</sub> is the area of the isosceles trapezoid; *S*<sub>3</sub> is the bottom corner area.

The spherical area *S*<sub>1</sub> is calculated as:

$$S_1 = \frac{\theta}{360} \pi R^2 - \frac{1}{2} R^2 \sin\theta \tag{3}$$

where,  $\theta$  is the center angle, °; *R* is the radius of the grooved wheel, mm.

The isosceles trapezoid area *S*<sub>2</sub> is given as:

$$S_2 = \frac{1}{2} h_1 \left( l + 2R \sin \frac{\theta}{2} \right) \tag{4}$$

where, *h*<sub>1</sub> is the trapezoidal height, given as:  $h_1 = h - R \left( 1 - \cos \frac{\theta}{2} \right)$ , mm; *l* is the length of the trapezoidal short side, given as:  $l = 2(R - h) \tan \frac{\theta}{2}$ , mm.

The bottom corner area *S*<sub>3</sub> is calculated as:

$$S_3 = 2r^2 \tan 2\psi - \frac{\psi}{360} \pi r^2 \tag{5}$$

where, *r* is the groove corner radius, mm;  $\psi$  is the groove corner angle ( $\psi = 90^\circ - \frac{\theta}{2}$ ), (°).

Equations (2)-(5) make it evident that *R*, *r*,  $\theta$ , and *h* have an impact on *S*. The groove radius *R* and spiral angle  $\theta$  are some of the main factors taken into account in this work. The value of *r* must be greater than the radius of the fertilizer particles, which was calculated to be 1.885 mm based on the size of the fertilizer particles employed in this study. Equation (6) provides the particular expression which relates the center angle  $\theta$  to both the spiral angle  $\alpha$  and the groove thickness *b*.

$$\theta = \frac{\pi}{4} - \frac{b}{R \sin \alpha} \tag{6}$$

After the fertilizer is filled into the groove of the grooved wheel, the motion of the grooved wheel is produced by the combination of axial translational motion and radial rotational motion along the grooved wheel. The spiral groove is extended, and the spiral line can be represented by a straight line. Figure 6 shows the force analysis of fertilizer particles at any point *M* in the spiral groove.

The fertilizer particles in the grooves are accelerated by a normal force *F*<sub>N</sub> at the point *M* in the spiral-normal direction. Friction *F*<sub>f</sub> is simultaneously produced as a result of the interaction

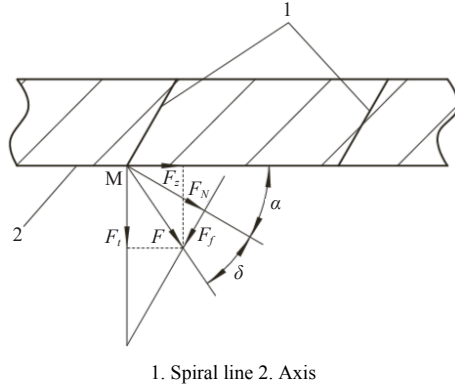


Figure 6 Force analysis of fertilizer particles in the grooves<sup>[34]</sup>

between the grooves and the fertilizer particles. Between the resultant force  $F$  and the normal thrust  $F_N$ , friction produces a deflection angle that is about similar to the fertilizer’s corresponding angle for external friction  $\delta$ . The following results are obtained by dividing the resultant force  $F$  into its axial force  $F_z$  and circumferential force  $F_t$  components:

The expression of each parameter is as follows<sup>[34]</sup>:

$$\begin{cases} F = \sqrt{F_z^2 + F_t^2} = \sqrt{F_f^2 + F_N^2} \\ F_z = F \cos(\alpha + \delta) \\ F_t = F \sin(\alpha + \delta) \end{cases} \quad (7)$$

where,  $F$  is the resultant force of the spiral groove acting on the fertilizer particles,  $N$ ;  $F_N$  is the normal force of the spiral groove on the fertilizer particles,  $N$ ;  $F_z$  is the axial force,  $N$ ;  $F_t$  is the circumferential force,  $N$ ;  $\alpha$  is the spiral angle of the spiral groove;  $\delta$  is the friction angle between the spiral groove and the fertilizer particles.

Similarly, the fertilizer particles of the spiral grooves are treated as the mass point  $m$ . The velocity analysis of this mass point is shown in Equation (8). The movement towards fertilizer particles of the spiral groove is driven by the fertilizer discharge shaft. The implicated velocity  $v_e$  is the linear velocity of the particles perpendicular to the axis direction, and the relative velocity  $v_r$  is parallel to the spiral direction. In the ideal case without considering friction, the absolute velocity is  $v_0$ . In reality, friction will cause the velocity due to friction  $v'$  to deviate from the ideal absolute velocity  $v_0$ . The deviation angle is  $\beta$ , and the actual absolute velocity after the deviation is  $v$ . At the same time, it can also be decomposed into circumferential velocity  $v_1$  and axial velocity  $v_2$ , which can be expressed as Equation (8)<sup>[43]</sup>.

$$\begin{cases} \vec{v}_0 = \vec{v}_e + \vec{v}_r \\ \vec{v} = \vec{v}_0 + \vec{v}' = \vec{v}_0 + \vec{v}' \end{cases} \quad (8)$$

The circumferential velocity  $v_1$  and axial velocity  $v_2$  decomposed from the actual absolute velocity  $v$  can be expressed as:

$$\begin{cases} v_1 = v \cos(\beta + \alpha) \\ v_2 = v \sin(\beta + \alpha) \end{cases} \quad (9)$$

Through trigonometric transformation, it can be obtained as:

$$\begin{cases} v_e = \omega l = \frac{\pi n l}{30}, v = \frac{v_0}{\cos \beta} = \frac{v_e \cos \alpha}{\cos \beta} \\ v_1 = \frac{\pi n l}{30} \frac{\cos \alpha}{\cos \beta} \cos(\beta), v_2 = \frac{\pi n l}{30} \frac{\cos \alpha}{\cos \beta} \sin(\beta + \alpha) \end{cases} \quad (10)$$

where,  $v_e$  is the implicated velocity, m/s;  $v_r$  is the relative velocity, m/s;  $v_0$  is the ideal absolute velocity, m/s;  $v'$  is the velocity due to

friction, m/s;  $v$  is the actual absolute velocity, m/s;  $v_1$  is the circumferential velocity, m/s;  $v_2$  is the axial velocity, m/s;  $n$  is the rotational speed of the double helix grooved wheel, r/min;  $\omega$  is the angular velocity of the double helix grooved wheel, rad/s;  $l$  is the distance between the fertilizer particle and the axis, mm;  $\beta$  is the angle at which the absolute velocity deviates from the theoretical velocity, ( $^\circ$ );  $\alpha$  is the spiral angle of the grooved wheel, ( $^\circ$ ).

According to the above equations, the velocity change of fertilizer particles in the spiral groove is related to the spiral angle of the groove, the distance between the fertilizer particles and the axis, and the rotation speed of the grooved wheel<sup>[34]</sup>.

### 2.3 Structural optimization of the spiral grooved wheel model

To optimize the effects of the spiral grooved wheel structural parameters on the fertilizer discharge performance, this study focused on four key structural and operational parameters: wheel speed, groove radius, wheel working length, and groove spiral angle as the test factors. By changing these key structural variables, orthogonal simulation experiments<sup>[43]</sup> were conducted to study the impact of these structural factors on fertilization performance. The diameter of the spiral grooved wheel was set at 48 mm, and the number of spiral grooves was 8. The levels of selected test factors are listed in Table 2.

Table 2 Test factor levels

Level	Wheel speed S/r·min <sup>-1</sup>	Groove radius R/mm	Wheel working length L/mm	Groove spiral angle $\alpha$ ( $^\circ$ )
1	20	5.5	20	45
2	30	6	30	50
3	40	6.5	40	55
4	50	7	50	60

#### 2.3.1 Simulation model setting

The simulation models of the fertilizer particles and discharge device were established, respectively. Urea granular fertilizer with a nitrogen content of 46% commonly used in Guangdong region was used. The shear modulus of the urea fertilizer was  $2.80 \times 10^7$  Pa, Poisson’s ratio was 0.25, density was 1337 kg/m<sup>3</sup>, and the particle spherical rate was greater than 90%. Since the sample’s overall evaluation suggested that the fertilizer particles have high spherical distribution characteristics, the spherical 3D model was chosen for the simulation<sup>[4,24,44,45]</sup> (Figure 7). In the simulation analysis, the default model of Hertz-Mindlin (no slip) was used for particles and particles, particles and discharge unit, and particles and soil because there was no binding effect between fertilizer particles. Combined with the test measurement and literature review<sup>[4,20,28,42]</sup>, the related physical and contact parameters of the fertilizer, discharge unit, and soil required for the simulation tests are listed in Table 3.

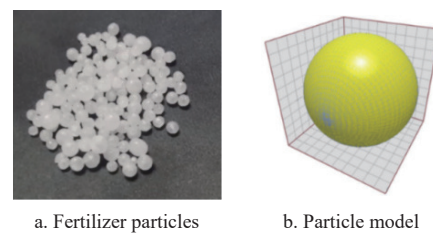


Figure 7 Fertilizer and its discrete element model

#### 2.3.2 Simulation test indicator

The coefficient of variation of fertilizer discharge uniformity was selected as the test evaluation index in this experiment. The simulation of the fertilizer discharge process of the spiral grooved wheel device was run under different test factors, as listed in Table 2.

The discharge mass rate of the device was recorded at every test factor level. The simulation was replicated five times for each test factor combination. Each simulation lasted for 3.5 s, and the mass of fertilizer discharged was recorded. The coefficient of variation of fertilizer discharge uniformity was assessed by the mean and standard deviation of discharged masses using Equations (11)-(13). Figure 8 shows the simulation process.

$$\bar{m} = \frac{1}{n} \sum m_i \tag{11}$$

$$s = \sqrt{\frac{1}{n-1} \sum (m_i - \bar{m})^2} \tag{12}$$

$$C_v = \frac{s}{\bar{m}} \times 100\% \tag{13}$$

where,  $\bar{m}$  is the average mass of fertilizer discharge, g;  $m_i$  is the mass of fertilizer discharge per unit time, g/s;  $n$  is the number of measurements;  $S$  is the standard deviation of the total mass of the fertilizer discharge, g;  $C_v$  is the coefficient of variation of fertilizer discharge, %.

**Table 3 Simulation test parameters**

Parameter	Density/ (kg·m <sup>-3</sup> )	Poisson's ratio	Shear modulus/ Pa	Restitution coefficient	Static friction coefficient	Rolling friction coefficient
Fertilizer-fertilizer	1.337	0.25	2.80×10 <sup>7</sup>	0.30	0.63	0.123
Fertilizer-steel	1.260	0.29	2.05×10 <sup>11</sup>	0.318	0.285	0.168
Fertilizer-soil	1.400	0.3	1.0×10 <sup>6</sup>	0.02	1.25	1.24

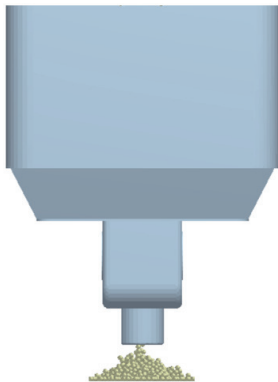


Figure 8 Fertilization simulation process

2.3.3 Spiral grooved wheel model verification test

The results of the aforementioned simulation test were used to create a structural model of the spiral-grooved wheel fertilizer discharge device. In five repeated tests, the actual fertilization effect was verified through the coefficient of variation of fertilizer discharge quantity. Figure 9 depicts the verification test setup.



Figure 9 Spiral grooved wheel model verification test

2.4 Simulation of fertilizer discharge accuracy of the single-row device

The fertilizer applicator designed in this paper is composed of six rows of fertilizer discharging units with the same specification, and the input power comes from the same source, so that the fertilizer discharging state of each row is consistent. To reduce the number of simulation calculations, the six-row fertilizer applicator was simplified into a single-row fertilizer device in the simulation environment, as presented in Figure 10.

2.4.1 Simulation test design

A soil layer with a length of 2500 mm and a width of 500 mm was set at a distance of 300 mm from the lower end of the fertilizer discharge outlet to represent the ground and accurately reflect the impact of the fertilizer discharge process on the soil. According to the agronomic requirements of rice fertilization in the Guangzhou area, the fertilizer application rate was set at 250 kg/hm<sup>2</sup>[26], and three different model speeds of the discharge wheel were set (30 r/min, 40 r/min, and 50 r/min, respectively). The ground speed ( $v=0.5$  m/s) was set for the simulation of the fertilizer discharge process. The simulation time was 3.5 s. A screenshot of the fertilization simulation process is shown in Figure 10.

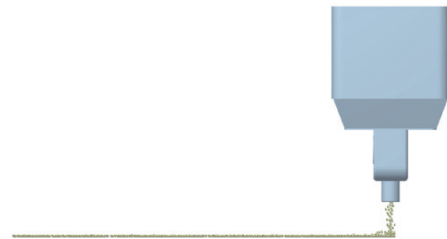


Figure 10 Simulation process for the single-row device

2.4.2 Performance indicators of the single-row device

The uniformity and accuracy of fertilizer discharge were selected as the performance evaluation indicators of the six-row fertilizer applicator in the simulation platform. The coefficient of variation of fertilizer discharge uniformity was used as an index to evaluate the accuracy of fertilization application. After the fertilizer discharge simulation tests, a sampling area of 1500 mm long was selected to determine the fertilizer discharge effect of the single-row device. The analyst function of DEM software was used to divide the sampling area into 5 identical bin grids, each with a size of 300 mm×200 mm×100 mm, as shown in Figure 11. The total mass of the fertilizer discharged in each sampling grid was measured, and the coefficient of variation ( $C_v$ ) of fertilizer discharge was calculated as follows<sup>[21]</sup>:

$$\bar{m} = \frac{\sum_{i=1}^n m_i}{n} \tag{14}$$

$$S = \sqrt{\frac{\sum_{i=1}^n (m_i - \bar{m})^2}{n-1}} \tag{15}$$

$$C_v = \frac{S}{\bar{m}} * 100 \tag{16}$$

where,  $\bar{m}$  is the average mass of fertilizer in the sampling grid, g;  $i$  is the sampling grid number;  $m_i$  is the mass of the fertilizer in the  $i$ -th grid, g;  $S$  is the standard deviation of fertilizer mass in all sampling grids, g; and  $C_v$  is the coefficient of variation of fertilizer discharge.



Figure 11 Simulation sampling area

The accuracy of fertilizer application was calculated using Equations (17) and (18)<sup>[21,26]</sup>.

$$A_r = 1 - \frac{|q_{r1} - q_{r2}|}{q_{r1}} \quad (17)$$

$$q_{r1} = \frac{1000Q_rWD}{15 \times 667 \times 6} \quad (18)$$

where,  $A_r$  is the application accuracy rate of fertilizer in the simulation test, %;  $Q_r$  is the required fertilizer application rate, kg/hm<sup>2</sup>;  $q_{r1}$  is the theoretical fertilizer discharged within the sampling area, g/s;  $q_{r2}$  is the simulated fertilizer discharged within the sampling area, g/s;  $W$  is the width of the six-row applicator, 1.8 m; and  $D$  is the sampling distance of simulation, 1.5 m.

**2.5 Consistency and stability tests of the 6RFA machine**

The consistency and stability of fertilizer discharge in each row are important indices for testing the working performance of fertilization machines<sup>[19,31,46]</sup>. The consistency of fertilizer output in each row of the fertilizer machine refers to the degree to which the fertilizer output in each row is consistent under the same conditions. The smaller the difference in the quantity of fertilizer discharged from each row, the better the consistency. The stability of fertilizer discharge refers to the degree to which the discharge capacity of the fertilizer machine is stable under the required conditions. The smaller the change in the total mass of fertilizer discharge each time, the better the stability of the fertilization machine. In this paper, a static test method was adopted to test the machine’s consistency and stability (Figure 12).



Figure 12 Static test of fertilization device

As shown in Figure 12, the experiment was carried out prior to the field test, and the fertilization machine was set up to keep it in a horizontal state. The control system drives the fertilizer discharge shaft to rotate at the normal operating speed, and the discharged fertilizers in each row are collected in plastic bags and weighed. The test was repeated five times; each test time was 20 s. The consistency and stability of fertilizer discharge were calculated using Equations (11)-(13).

**2.6 Field test of the 6RFA**

**2.6.1 Test site**

The field test of the 6RFA was conducted at Shapu Experimental Farm of Zhaoqing Agricultural Research Institute in Zhaoqing City, Guangdong Region, China (23°15’N, 112°65’E with 17 m of elevation). The soil texture was sandy loam. Generally, this

region has a sub-tropical and monsoon-type climate<sup>[47]</sup>. The tests were carried out according to the Technical Specification for Quality Evaluation of Fertilization Machinery in China (NY/T1003-2006)<sup>[32]</sup>.

**2.6.2 Experimental plan**

The experiment was divided into five plots, each measuring 2.5 m by 25 m. The expected application rates for the applicator were set at 150 kg/hm<sup>2</sup>, 225 kg/hm<sup>2</sup>, 300 kg/hm<sup>2</sup>, and 375 kg/hm<sup>2</sup>, respectively. These rates are within the required fertilization rates for rice crops in Guangdong Province<sup>[32,48]</sup>. The total mass of fertilizer in the fertilizer box before and after the test were recorded, and we then used Equation (19) to calculate the deviation of the total amount of fertilizer applied in the test area. The field test setup for fertilization accuracy is shown in Figure 13.



Figure 13 Field test of the 6RFA machine

**2.6.3 Fertilization accuracy**

The fertilization accuracy of the developed fertilizer applicator was evaluated based on the expected fertilization rates of rice crops, ranging from 150 to 400 kg/hm<sup>2</sup><sup>[32,47]</sup>. The deviation of fertilization rate per row ( $\gamma_s$ ) was used to evaluate the accuracy of fertilization. The deviation of the total amount of fertilizer applied by the fertilizer applicator refers to the absolute ratio of the difference between the actual and expected application rates, expressed as follows<sup>[32]</sup>:

$$\gamma_s = \frac{\left| \frac{10000(W_b - W_a)}{S} - F \right|}{F} \times 100 \quad (19)$$

where,  $W_b$  is the mass of fertilizer added to the fertilizer box at the beginning of the test, kg;  $W_a$  is the mass of residual fertilizer in the fertilizer box at the end of the test, kg;  $S$  is the operation area, m<sup>2</sup>;  $F$  is the expected amount of fertilizer, kg/hm<sup>2</sup>.

**3 Results and discussion**

**3.1 Optimization model results of the spiral grooved wheel structure**

In order to test the influence of the selected factors on the coefficient of variation of fertilizer discharge, an L16(4) orthogonal experimental design was generated in SPSS software. Table 4 lists the orthogonal simulation results and the influence of the selected test factors on the coefficient of variation of fertilizer discharge quantity.

The results of the simulation test show that the optimum structural parameters of the spiral grooved wheel fertilizer application device are: the grooved wheel rotation speed of 40 r/min, the groove section radius of 6 mm, the grooved wheel working length of 50 mm, and the grooved wheel spiral angle of 45°. The coefficient of variation of fertilizer discharge uniformity under these parameter settings was 5.58% (Table 4). Many scholars have confirmed that operating the spiral grooved wheel fertilization model under these structural parameters produces the smallest

coefficient of variation in fertilization quantity<sup>[19,28,36,43]</sup>. To further understand the importance of these test parameters of the spiral grooved wheel device on the discharge performance, a variance analysis of the test results was carried out, and Table 5 presents the results.

**Table 4 Experimental design and results**

Test No.	<i>S</i>	<i>R</i>	<i>L</i>	$\alpha$	Coefficient of variation of fertilization uniformity/%
1	1	1	1	1	8.58
2	1	2	2	2	15.75
3	1	3	3	3	13.94
4	1	4	4	4	8.63
5	2	1	2	4	14.04
6	2	2	1	3	8.71
7	2	3	4	2	7.72
8	2	4	3	1	12.36
9	3	1	3	2	14.64
10	3	2	4	1	5.58
11	3	3	1	4	10.39
12	3	4	2	3	15.24
13	4	1	4	3	6.36
14	4	2	3	4	8.93
15	4	3	2	1	9.7
16	4	4	1	2	7.67
$\sigma_1$	11.725	10.905	8.838	9.055	
$\sigma_2$	10.708	9.743	13.683	11.445	
$\sigma_3$	8.165	10.438	12.468	11.063	
$\sigma_4$	11.463	10.975	7.073	10.498	
Optimal parameters	$S_3R_2L_4\alpha_1$				

It can be seen from Table 5 that the working length of the spiral grooved wheel had a very significant impact on the fertilizer discharge performance, while the rotating speed of the grooved wheel had a significant effect. The spiral angle and the section radius of the grooved wheel had no significant impact on the fertilizer discharge performance. Wang et al.<sup>[19]</sup> observed similar results, but Zhang et al.<sup>[36]</sup> found that the spiral angle of the spiral grooved wheel had a significant impact on the uniformity of fertilizer discharged.

The variation coefficient of fertilizer discharge uniformity assessed through the verification test was 5.95% after five consecutive tests. The verification results had a slightly higher coefficient of variation than that of the simulation test (5.58%). The

error between the simulation and the experimental results was 6.30%. Therefore, it can be confirmed that the simulation and the verification test results are essentially consistent. The results further validate the reliability of using discrete element simulation method to study the fertilizer discharge process of the spiral grooved wheel device designed in this paper.

**Table 5 Analysis of variance**

Source of variation	Deviation sum of squares	Df	Sum of mean squares	<i>F</i>	Significance
<i>S</i>	32.886	3	11.762	3.603	*
<i>R</i>	5.066	3	2.489	1.493	
<i>L</i>	115.241	3	39.214	9.848	**
$\alpha$	4	3	2.133	1.415	
Error	14.386	3			

Note: \*Significant; \*\*Very significant at the 5% level by LSD

**3.2 Fertilization accuracy results of the single-row device**

According to the agronomic requirements of rice fertilization in the Guangzhou area, the fertilizer application rate was set at 250 kg/hm<sup>2</sup>, and three different model speeds of the discharge wheel were set (30 r/min, 40 r/min, and 50 r/min, respectively). The accuracy of fertilizer application was calculated using Equations (17) and (18) in this paper. The simulation test results and analysis for the single-row discharge device in a typical field environment are listed in Table 6.

From the results in Table 6, it can be seen that the coefficient of variation of fertilizer discharge uniformity decreases with the increase in rotation speed, and the accuracy of fertilizer discharge first decreases and then increases with the increase in rotation speed of the discharge wheel. However, this trend changed as the speed increased to 50 r/min. When the rotation speed was 30 r/min, the coefficient of variation of fertilizer discharge uniformity was the largest (21.90%), and the accuracy of fertilizer discharge was the lowest (61.8%). When the speed was 40 r/min, the accuracy of fertilization was the highest (90.4%), and the coefficient of variation of fertilizer discharge uniformity was the lowest (8.42%). When the rotation speeds of the fertilizer discharge wheel were 40 r/min and 50 r/min respectively, the uniformity of fertilizer discharge was better, and the difference in coefficient of variation was smaller. In addition, the accuracy of fertilizer discharge was high, and the difference in accuracy between the two rotational speeds was small. Therefore, the simulation model had good fertilizer discharge performance at 40 r/min. Many researchers have also found that fertilizer discharge devices with spiral grooves operate well between 35-50 r/min<sup>[4,26,28,34-36,43]</sup>.

**Table 6 Simulation results and analysis of fertilizer application device**

Speed/(r·min <sup>-1</sup> )	<i>q<sub>r1</sub></i> /g	Amount of fertilizer in the sampling box/g					Total/g	Mean/g	<i>S<sub>σ</sub></i>	<i>C<sub>v</sub></i>	<i>A<sub>r</sub></i> /%
		1	2	3	4	5					
30	13.49	4.52	3.05	4.91	3.15	3.01	18.64	3.73	0.82	21.90	61.8
40	13.49	3.04	3.12	3.15	2.47	3.00	14.78	2.96	0.25	8.42	90.4
50	13.49	3.05	3.11	3.83	3.6	2.94	16.53	3.31	0.35	10.47	77.5

**3.3 Static test results of the 6RFA**

The consistency and stability test results of fertilizer discharge in each row are listed in Table 7. Based on the experimental results, the standard deviation and coefficient of variation for the consistency and stability of fertilizer output in each row were calculated using Equations (11)-(13). The consistency variation coefficient (*C<sub>v</sub>*) of the fertilizer discharge amount in each row was calculated to be 4.41%, which is within the range of 13.0% of the

qualified evaluation index of fertilizer machinery and tools in China<sup>[32,36]</sup>. Therefore, the discharge volume of each row of the deep fertilization machine designed in this paper had good consistency. The variation coefficient *C<sub>v</sub>* of fertilizer discharge stability in each row was calculated to be 2.53%, which is within the range of 7.8% of the qualified evaluation index of fertilizer machinery and tools. Therefore, the total fertilizer discharged by the deep fertilization device was stable. In addition, the *C<sub>v</sub>* of the amount of fertilizer in

each row ranged from 1.13% to 5.95%, which meets the requirement of a  $C_v$  less than 13%<sup>[32,36]</sup>. The test results and analysis are listed in Table 7.

**3.4 Field test results**

Figure 14 compares the expected and measured fertilization rates of the 6RFA. It was observed that measured fertilization rates were slightly higher than the expected fertilization rates when the required fertilization rates were 150 kg/hm<sup>2</sup>, 225 kg/hm<sup>2</sup>, and 300 kg/hm<sup>2</sup>, while the measured fertilization rate was lower when the required fertilization rate was set at 375 kg/hm<sup>2</sup>. This may be because, in order to increase the amount of fertilizer discharge while maintaining a consistent working speed, the motor speed must be increased. The amount of fertilizer applied by the fertilizer

discharge device in a single turn will, however, decrease as the motor speed increases, resulting in a decrease in fertilization rate. Similar findings were reported by Shi et al.<sup>[32]</sup>

**Table 7 Fertilizer discharge in static test**

Row	Fertilizer discharge/g					Mean	S	$C_v$
	1	2	3	4	5			
1	298	301	293	301	300	298.6	3.36	1.13
2	292	292	295	285	293	291.4	3.78	1.30
3	321	312	310	314	312	313.8	4.27	1.36
4	309	296	302	295	305	301.4	5.94	1.97
5	276	270	282	279	296	280.6	9.69	3.45
6	275	275	315	294	302	292.2	17.40	5.95

Note: S = Standard deviation;  $C_v$  = Coefficient of variation

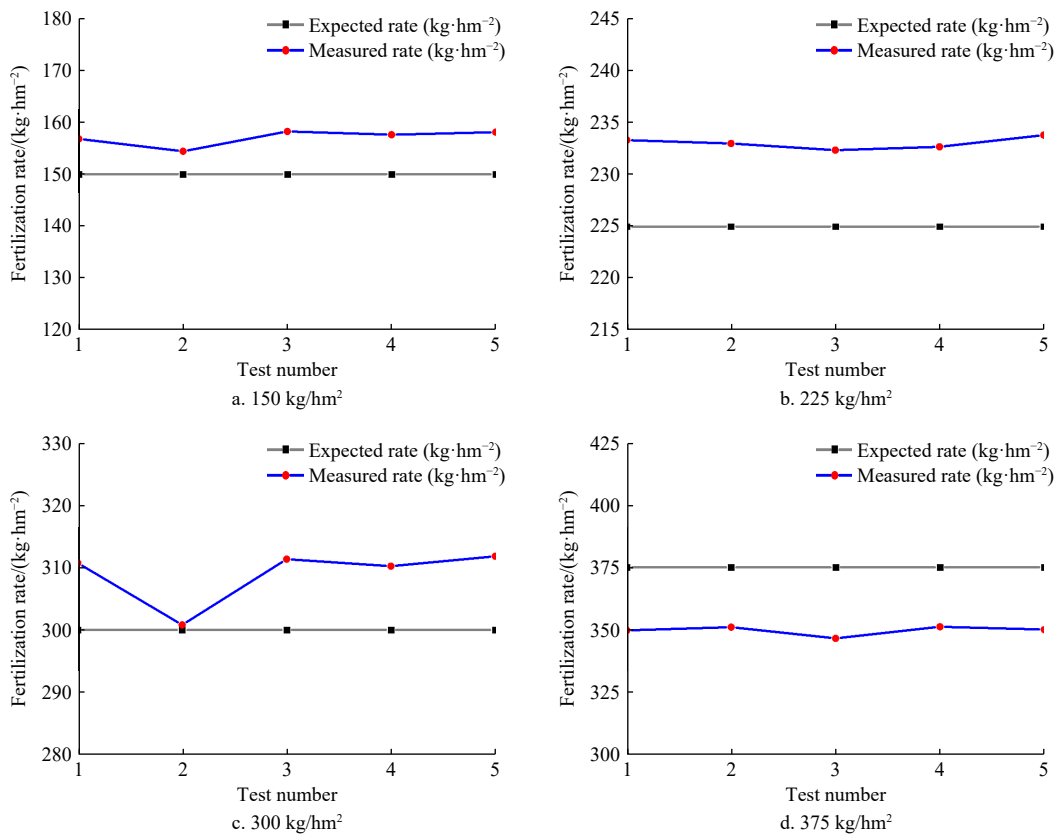


Figure 14 Expected versus measured fertilization rates for target values

Table 8 shows the deviation of measured fertilization rates from expected rates. When the expected fertilization rates were 150 kg/hm<sup>2</sup>, 225 kg/hm<sup>2</sup>, 300 kg/hm<sup>2</sup>, and 375 kg/hm<sup>2</sup>, the deviation ranges of the measured fertilization rates were 2.85%-5.11%, 3.28%-3.75%, 0.27%-3.80%, and 6.35%-7.58%, respectively, with an overall average of 4.5%. The machine’s application accuracy meets the design standards, and the deviation of less than 15% meets the fertilization requirements. Similar  $C_v$ ’s and deviation trends were earlier reported in the literature<sup>[32,33]</sup>. This proves that the uniformity

**Table 8 Deviation of measured fertilization rates from expected rates**

Expected rate/ (kg·hm <sup>-2</sup> )	Deviation of fertilization rate per row $\gamma_s$ /%					Average
	1	2	3	4	5	
150	4.34	2.85	5.21	4.82	5.11	4.47
225	3.55	3.42	3.15	3.28	3.75	3.43
300	3.45	0.27	3.65	3.30	3.80	2.89
375	6.73	6.39	7.58	6.35	6.65	7.23

and accuracy of the developed prototype fertilization machine were worth verifying, with a fertilization accuracy of 95.5%.

**4 Conclusions**

In order to improve the efficiency and quality of rice fertilization and reduce agricultural non-point source pollution, a six-row deep fertilizer applicator was developed with a spiral grooved wheel model. Through discrete element simulation and testing, the structural parameters of the spiral grooved wheel were optimized. The effects of the rotating speed, groove radius, grooved wheel working length, and spiral angle of the groove on the uniformity of fertilizer discharge were studied, and the optimum structural parameters of the spiral grooved wheel were obtained. The use of the spiral grooved wheel can improve the fertilizer discharge effect.

At the same time, the performance of the 6RFA machine was investigated under static and field conditions. According to the performance testing of the machine under static conditions, the consistency and stability changes of each row of fertilizers were less

than 5%. The simulation and field test results show that the uniformity and accuracy of fertilizer application with the 6RFA machine are very high. Under the field test, the deviation of fertilization amount per row was between 2.89% and 7.23% from all the expected application rates, and the corresponding average deviation of fertilization rates was less than 5%. The proposed deep fertilizer applicator meets all the requirements of the Technical Specification for Quality Assessment of Fertilization Machinery in China (NY/T1003-2006). These results will provide a reference basis for selecting the best fertilizer discharge device and guiding the design of high-performance fertilizer applicators. However, further exploration of the structural parameters of the spiral grooved wheel is needed to investigate the influence of groove depth, groove thickness, groove pitch, and other parameters on fertilizer discharge effect.

## Acknowledgements

This research was financially supported by the National Key Research and Development Plan of China (Grant No. 2023YFD1701004), Earmarked Fund for Modern Agro-industry Technology Research System in China (Grant No. CARS-01-02A), and the Specific University Discipline Construction Project (Grant No. 2023B10564002).

## [References]

- [1] Qiang S C, Zhang Y, Zhao H, Fan J L, Zhang F C, Sun M, et al. Combined effects of urea type and placement depth on grain yield, water productivity and nitrogen use efficiency of rain-fed spring maize in northern China. *Agricultural Water Management*, 2022; 262: 107442.
- [2] Zhou H, Zhou T N, Wang X Z, Hu L, Wang S S, Luo X W, et al. Determination of discrete element modelling parameters of a paddy soil with a high moisture content (>40%). *Agriculture*, 2022; 12: 2000.
- [3] Shi Y Y, Hu Z C, Wang X C, Odhiambo M O, Sun G X. Fertilization strategy and application model using a centrifugal variable-rate fertilizer spreader. *Int J Agric & Biol Eng*, 2018; 11(6): 41–48.
- [4] Bangura K, Gong H, Deng R L, Tao M, Liu C, Cai Y H, et al. Simulation analysis of fertilizer discharge process using the discrete element method (DEM). *PLoS ONE*, 2020; 15: e0235872.
- [5] Li X, Wu T Y, Li Y S, Hu X, Wang Z X, Liu J F, et al. Deep fertilization improves rice productivity and reduces ammonia emissions from rice fields in China; a meta-analysis. *Field Crops Research*, 2022; 289: 108704.
- [6] Wu P, Liu F, Chen G Z, Wang J Y, Huang F Y, Cai T, et al. Can deep fertilizer application enhance maize productivity by delaying leaf senescence and decreasing nitrate residue levels? *Field Crops Research*, 2022; 277: 108417.
- [7] Zhong X M, Peng J W, Kang X R, Wu Y F, Luo G W, Hu W F, et al. Optimizing agronomic traits and increasing economic returns of machine-transplanted rice with side-deep fertilization of double-cropping rice system in southern China. *Field Crops Research*, 2021; 270: 108191.
- [8] Wang X, Wang Y L, Zhang Y P, Xiang J, Zhang Y K, Zhu D F, et al. The nitrogen topdressing mode of indica-japonica and indica hybrid rice are different after side- deep fertilization with machine transplanting. *Scientific Reports*, 2021; 11: 1494.
- [9] Nishith R P, Damodar J, Rabi N S. Drivers in adoption of urea deep placement technology in paddy cultivation: An empirical study in Kalahandi District of Odisha, India. *Journal of Agriculture and Crops*, 2023; 9(2): 164–171.
- [10] Wu P, Zhao G, Huang H, Wu Q, Bangura K, Cai T, et al. Optimizing soil and fertilizer management strategy to facilitate sustainable development of wheat production in a semi-arid area: A 12-year in-situ study on the Loess Plateau. *Field Crops Research*, 2023; 302: 109084.
- [11] Nasielski J, Grant B, Smith W N, Caleb N, Ken J, Bill D. Effect of nitrogen source, placement and timing on the environmental performance of economically optimum nitrogen rates in maize. *Field Crops Research*, 2020; 246: 107686.
- [12] Chen T, Shi Z, Wen A, Li L N, Wang W K. The role of paddy fields in the sediment of a small agricultural catchment in the Three Gorges Reservoir Region by the sediment fingerprinting method. *Land*, 2023; 12: 875.
- [13] Chen M, Yang Z J, Wang X C, Shi Y Y, Zhang Y. Response characteristics and efficiency of variable rate fertilization based on spectral reflectance. *Int J Agric & Biol Eng*, 2018; 11(6): 152–158.
- [14] Li L, He L X, Li Y Q, Wang Y F, Ashraf U, Hamoud Y A, et al. Deep fertilization combined with straw incorporation improved rice lodging resistance and soil properties of paddy fields. *European Journal of Agronomy*, 2023; 142: 126659.
- [15] Deng S Y, Ashraf U, Nawaz M, Abbas G, Tang X R, Mo Z W. Water and nitrogen management at the booting stage affects yield, grain quality, nutrient uptake, and use efficiency of fragrant rice under the agro-climatic conditions of South China. *Frontiers in Plant Science*, 2022; 13: 907231.
- [16] Chen Z M, Wang Q, Ma J W, Zou P, Jiang L N. Impact of controlled-release urea on rice yield, nitrogen use efficiency and soil fertility in a single rice cropping system. *Scientific Reports*, 2020; 10: 10432.
- [17] Chen G Z, Wu P, Wang J Y, Zhou Y D, Ren L Q, Cai T, et al. How do different fertilization depths affect the growth, yield, and nitrogen use efficiency in rain-fed summer maize? *Field Crops Research*, 2023; 290(2): 108759. doi: 10.1016/j.fcr.2022.108759
- [18] Yokamo S, Jiao X Q, Jasper K, Fekadu G, Mohammad S J, Rongfeng J. Grain yield and nitrogen use efficiency vary with cereal crop type and nitrogen fertilizer rate in Ethiopia: A meta-analysis. *Agricultural Sciences*, 2022; 13: 612–631.
- [19] Wang X Y, Tang Y R, Lan H P, Liu Y, Zeng Y, Tang Z H, et al. Performance analysis and testing of spiral quantitative fertilizer distributors in orchards. *Applied Sciences*, 2023; 13: 8941.
- [20] Bu H R, Yu S Y, Dong W C, Zhang L X, Xia Y Q. Analysis of the effect of bivariate fertilizer discharger control sequence on fertilizer discharge performance. *Agriculture*, 2022; 12(11): 1927.
- [21] Zhang X L, Pei Y K, Chen Y, Song Q L, Zhou P L, Xia Y Q, et al. The design and experiment of vertical variable cavity base fertilizer fertilizing apparatus. *Agriculture*, 2022; 12(11): 1793.
- [22] Gao Y Y, Feng K Y, Yang S, Han X, Wei X H, Zhu Q Z, et al. Design and experiment of an unmanned variable-rate fertilization control system with self-calibration of fertilizer discharging shaft speed. *Agronomy*, 2024; 14: 2336.
- [23] Gao X J, Xie G F, Xu Y, Yu Y B, Lai Q H. Application of a staggered symmetrical spiral groove wheel on a quantitative feeding device and investigation of particle motion characteristics based on DEM. *Powder Technology*, 2022; 407: 117650.
- [24] Dun G Q, Gao Z Y, Liu Y X, Ji W Y, Mao N, Wu X P, et al. Optimization design of fertilizer apparatus owned arc gears based on discrete element method. *Int J Agric & Biol Eng*, 2021; 14(2): 97–105.
- [25] Zha X T, Zhang G Z, Zhang S J, Hou Q X, Wang Y, Zhou Y. Design and experiment of centralized pneumatic deep precision fertilization device for rice transplanter. *Int J Agric & Biol Eng*, 2020; 13(6): 109–117.
- [26] He Y K, Li C L, Zhao X G, Gao Y Y, Li S, Wang X. Simulation analysis of the fertilizer ejecting device of corn fertilizer applicator based on EDEM. *Journal of Physics: Conference Series*, 2020; 1633: 0120612020.
- [27] Ahmad F, Qiu B J, Ding Q S, Ding W M, Khan Z M, Shoaib M, et al. Discrete element method simulation of disc type furrow openers in paddy soil. *Int J Agric & Biol Eng*, 2020; 13(4): 103–110.
- [28] Chen H B, Zheng J F, Lu S J, Zeng S, Wei S L. Design and experiment of vertical pneumatic fertilization system with spiral Geneva mechanism. *Int J Agric & Biol Eng*, 2021; 14(4): 135–144.
- [29] Qi J T, Tian X L, Li Y, Fan X H, Yuan H F, Zhao J L, et al. Design and experiment of a subsoiling variable rate fertilization machine. *Int J Agric & Biol Eng*, 2020; 13(4): 118–124.
- [30] Zhou W Q, Wang J W, Tang H. Structure optimization of cam executive component and analysis of precisely applying deep-fertilization liquid fertilizer. *Int J Agric & Biol Eng*, 2019; 12(4): 104–109. 10.25165/ij. ijabe. 20191204.4865
- [31] Adilet S, Zhao K Y, Liu G Y, Sayakhat N, Chen J, Hu G R, et al. Investigation of the pin-roller metering device and tube effect for wheat seeds and granular fertilizers based on DEM. *Int J Agric & Biol Eng*, 2023; 16(2): 103–114.
- [32] Shi Y, Xi X, Gan H, Shan X, Zhang Y, Shen H, Zhang R. Design and Experiment of Row-Controlled Fertilizing–Weeding Machine for Rice Cultivation. *Agriculture*, 2021; 11: 527.
- [33] Zeng S, Tang H, Luo X, Ma G, Wang Z, et al. Design and experiment of precision rice hill-drop drilling machine for dry land with synchronous fertilizing. *Transactions of the CSAE*, 2012; 28(20): 12–19.

- [34] Wang J F, Fu Z D, Jiang R, Song Y L, Yang D Z, Wang Z T. Influences of grooved wheel structural parameters on fertilizer discharge performance: Optimization by simulation and experiment. *Powder Technology*, 2023; 418: 118309.
- [35] Yan D, Xu T, Yu J, Wang Y, Guan W, Tian Y, Zhang N. Test and simulation analysis of the working process of soybean seeding monomer. *Agriculture*, 2022; 12: 1464.
- [36] Zhang L P, Zhang L X, Zheng W Q. Fertilizer feeding mechanism and experimental study of a spiral grooved-wheel fertilizer feeder. *Journal of Engineering Science and Technology Review*, 2018; 11(6): 107–115.
- [37] Przywara A, Santoro F, Kraszkiewicz A, Anna P, Simone P. Experimental study of disc fertilizer spreader performance. *Agriculture*, 2020; 10: 467.
- [38] Shen C J, Zhang L X, Jia S X, Zhou Y, Li F, Dai Y M, et al. Parameter optimization and test of hydraulic soil insertion device of orchard gas explosion subsoiling and fertilizing machine. *Int J Agric & Biol Eng*, 2023; 16(2): 132–141.
- [39] Zeng S, Tan Y P, Wang Y, Luo X W, Yao L M, Huang D P, et al. Structural design and parameter determination for fluted-roller fertilizer applicator. *Int J Agric & Biol Eng*, 2020; 13(2): 101–110.
- [40] Feng Y L, Yin X C, Jin H R, Tong W Y, Ning X F. Design and experiment of a Chinese chive harvester. *Int J Agric & Biol Eng*, 2023; 16(2): 125–131.
- [41] Shao Y Y, Zhang H D, Xuan G T, Zhang T, Guan X L, Wang F H. Simulation and experiment of a transplanting mechanism for sweet potato seedlings with ‘boat bottom’ transplanting trajectory. *Int J Agric & Biol Eng*, 2023; 16(3): 96–101.
- [42] Liu X P, Niu Z J, Li M, Hou M X, Wei L J, Zhang Y, et al. Design and experimental research on disc-type seeding device for single-bud sugarcane seeds. *Int J Agric & Biol Eng*, 2023; 16(2): 115–124.
- [43] Wang Y B, Liang F, Xu F, Deng W H, Yu Y Z. Discrete element simulation and experiment of opposed double helix outer sheave fertilizer discharger. *INMATEH-Agricultural Engineering*, 2022; 68(3): 617–628.
- [44] Xu T Y, Zhang R X, Zhu F W, Feng W Z, Wang Y, Wang J L. A DEM-based modeling method and simulation parameter selection for cyperus esculentus seeds. *Processes*, 2022; 10: 1729.
- [45] Liu J S, Gao C Q, Nie Y J, Yang B, Ge R Y, Xu Z H. Numerical simulation of Fertilizer Shunt-Plate with uniformity based on EDEM software. *Computers and Electronics in Agriculture*, 2020; 178: 105737.
- [46] Zhang M Q, Tang Y R, Zhang H, Lan H P, Niu H. Parameter optimization of spiral fertilizer applicator based on artificial neural network. *Sustainability*, 2023; 15(3): 1744.
- [47] Wehmeyer H, Annalyn H G, Melanie C. Reduction of fertilizer use in south china—impacts and implications on smallholder rice farmers. *Sustainability*, 2020; 12: 2240.
- [48] Ding S P, Bai L, Yao Y X, Yue B, Fu Z L, Zheng Z Q, et al. Discrete element modelling (DEM) of fertilizer dual-banding with adjustable rates. *Computers and Electronics in Agriculture*, 2018; 152: 32–39.